Conclusions

The manganese activated $ZnGa_2O_4$ phosphor was prepared by the polymerized complex method to improve the photoluminesence properties of the phosphor. The $ZnGa_2O_4$: Mn phosphor prepared by this method shows a remarkable increase in the emission intensity than that prepared by conventional method. Therefore, the polymerized complex method is an available process for the preparation of phosphor since homogeneous particles in a small size level can be easily prepared without pulverizing process. Also, the increase in emission intensity after a reducing firing is a result of the conversion of the highly oxidized manganese (IV) to Mn^{2+}.

Acknowledgment. This research was supported financially by the Ministry of the Science and Technology in Korea.

References

1. (a) Kobayashi, H.; Tanaka, S. *Journal of the SID* **1996**, *4/3*, 157. (b) Minami, T.; Maeno, T.; Kuroi, Y.; Takata, S. *Jpn. J. Appl. Phys.* **1995**, *34*, L684. (c) Minami, T.; Takata, S.; Kuroi, Y. *SID Intl. Symp. Digest Tech. Papers* **1995**, 724.
2. Yamamoto, H. *Journal of the SID* **1996**, *4/3*, 165.
3. Pechini, M. P. *U.S. Patent* **1967**, *July No.3*, 330, 697.
4. (a) Anderson, H. U.; Pennell, M. J.; Guha, J. P. *Advances in Ceramics, Ceramic Powder Science*; edited by Messing, G. L.; Mazdiyasni, J. W.; McCauley & R. A. Haber (Am. Ceram. Soc. 21 Westerville OH, 1987), p 91. (b) Lessing, P. A. *Am. Ceram. Soc. Bull.* **1989**, *168*, 1002. (c) Tai, L. W.; Lessing, P. A. *J. Mater. Res.* **1992**, *7*, 511. (d) Cho, S. G.; Johnson, P. F.; Condrate, R. A. *J. Mater. Sci.* **1990**, *25*, 4738. (e) Kakihana, M.; Borjesson, L.; Eriksson, S.; Svedlindh, P. *J. Appl. Phys.* **1991**, *69*, 867. (f) Kakihana, M.; Yoshimura, M.; Mazaki, H.; Yasuoka H.; Borjessen *J. Appl. Phys.* **1992**, *71*, 3904. (g) Berastegui, P.; Kakihana, M.; Yoshimura, M.; Mazaki, H.; Yasuoka, H.; Johanssen, L. G.; Eriksson, S.; Borjessen, L.; Kall, M. *J. Appl. Phys.* **1993**, *73*, 2424.
5. Hsieh, I. J.; Chu, K. T.; Yu, C. F.; Feng, M. S. *J. Appl. Phys.* **1994**, *76*, 3735.
6. Shmulovich, J.; Kocian, D. F. *Proc. SID.* **1989**, *30*, 200.
7. (a) Itoh, S.; Kimizuka, T.; Tonegawa, T. *J. Electrochem. Soc.* **1989**, *138*, 1819. (b) Itoh, S.; Toki, H.; Sato, Y.; Morimoto, K.; Kishino, T. *J. Electrochem. Soc.* **1991**, *138*, 1509.
8. JCPDS data file, **1986**, No. 3-1155.
9. Jo, D.-H.; Jung, H.-K.; Kim, C.-H.; Seok, S.-I.; Park, D.-S. *J. Kor. Chem. Soc., manuscript for publication.*
10. Jpn, Phosphor Research Society, Phosphor handbook, 1987.
11. Chang, I. F.; Brownlow, J. W.; Sun, T. I.; Wilson, J. S. *J. Electrochem. Soc.* **1989**, *136*, 3532.
12. Morell, A.; El Khiati, N. *J. Electrochem. Soc.* **1993**, *140*, 2019.
13. Kutty, T. R. N.; Devi, L. G. *Mater. Res. Bull.* **1986**, *21*, 1093.

Preparation and Characterization of $LiMn_2O_4$ Powder by Combustion of Poly(ethylene glycol)-Metal Nitrate Precursor

Hyu-Bum Park, Young-Sik Hong, Ji-Eun Yi*, Ho-Jin Kweon, and Si-Joong Kim†**

Department of Chemistry, Korea University, Sungbuk-Gu, Seoul 136-701, Korea
**Korea Basic Science Institute, Sungbuk-Gu, Seoul 136-701, Korea*
***Samsung Display Devices Co., Hwasung-Gun, Kyungki-Do 445-970, Korea*
Received February 25, 1997

$LiMn_2O_4$ powders were prepared by burning and subsequent calcination of PEG-metal nitrate precursor. After the burning stage of the precursor, some minor phases such as Mn_2O_3 (or Mn_3O_4), MnO, and carbonate were formed and single phases of $LiMn_2O_4$ were obtained by further calcinations above 400 °C. From thermal analysis of the precursor, a violent thermal decomposition, which was indicated by a drastic weight loss accompanied by a sharp and strong exothermic peak, was observed and probably caused by an oxidation-reduction reaction between oxidizer and fuel. The formation of the minor phases could be explained in terms of the burning behavior of the precursor by employing valence concepts of propellant chemistry. The calcined powders were composed of submicron-sized but highly agglomerated particles and showed very broad particle size distribution.

Introduction

The spinel $LiMn_2O_4$ and the layered compounds $LiCoO_2$ and $LiNiO_2$ are the most widely studied cathode materials for Li ion rechargeable batteries.[1,2] Among these lithium transition metal oxides, $LiMn_2O_4$ has attracted a good deal of research because of its economical and environmental advantages; Mn is abundant and significantly cheaper than Co

†To whom correspondence should be addressed

and Ni, and $LiMn_2O_4$ is the least toxic among these compounds.

Preparation of $LiMn_2O_4$ has been usually carried out in a solid-state reaction.[3-5] In this method, a Mn compound, such as MnO_2, Mn_2O_3, or $MnCO_3$, is first mixed with a Li compound, such as $LiNO_3$, LiOH, or Li_2CO_3, in the molar ratio of 2Mn : 1Li. After extensive grinding and mixing, the resultant mixture is calcined in air at high temperatures, *e.g.*, 750 to 900 °C, for an elongated period. In addition, solution methods using soluble Li and Mn sources have been also developed.[6-8] The latter offers a starting materials with much better homogeneity between the Li and Mn components and yields $LiMn_2O_4$ at lower calcination temperature. Among the solution methods, techniques based on using organic polymers as a gelling and complexing agent have been developed by some investigators and used to produce mixed-cation oxide powders. In 1967, Pechini[9] invented a simple powder preparation process using polyester polymeric precursors. Thereafter, other polymers, such as PEG (poly(ethylene glycol)),[10,11] PVA (poly(vinyl alcohol)),[12,13] and PAA (poly(acrylic acid)),[14-17] have been used to prepare metal oxides. Recently, the lithium transition metal oxides have been successfully synthesized through the polymeric precursors. For example, Sun *et al.*[17] have prepared ultrafine $LiCoO_2$ powders by using PAA, and Liu *et al.*[8] have also reported the electrochemical applications of $LiMn_2O_4$ powders synthesized by the Pechini process.

Patil's group[18-21] have prepared very fine metal oxide powders by using a simple and rapid *in situ* combustion process. They applied concepts[22] employed in propellant chemistry to the preparations of metal oxide powders. In this process, the elements from the reactants were considered as a fuel or an oxidizer and an auto-ignited oxidation-reduction reaction could occur in the course of combustion of the precursor. Park *et al.*[11] have reported preparation of $La_{1-x}Sr_xMnO_3$ powder by *in situ* auto-ignited combustion of polymeric precursors and applied the concepts to explain the formation route of perovskite phase and the characteristics of the obtained powder.

In the present study, we report on the preparation of $LiMn_2O_4$ powder by the combustion of PEG-metal nitrate gel precursor. The formation route of $LiMn_2O_4$ from the precursor was studied by thermal analysis, X-ray diffraction, and FT-IR spectroscopy. In order to explain the formation route of $LiMn_2O_4$ we used the valence concepts, which are normally applied in propellant chemistry. In addition, the characteristics of powders prepared by this process were also investigated by several methods, such as scanning electron microscopy, elemental analysis, and particle size analysis.

Experimental

$LiNO_3$ (Junsei, EP), $Mn(NO_3)_2 \cdot xH_2O$ (Yakuri, GR), and PEG (Yakuri, EP; average molecular weight=2.0×10^4) were used as the starting materials. In order to determine the content of Mn in $Mn(NO_3)_2 \cdot xH_2O$, a stock solution of $Mn(NO_3)_2$ was prepared and standardized by EDTA titration. The preparation route of $LiMn_2O_4$ powder is schematically illustrated in Figure 1.

PEG-metal nitrate precursor was prepared as follows. Initially, stoichiometric amounts of $LiNO_3$ (0.03 mol) and

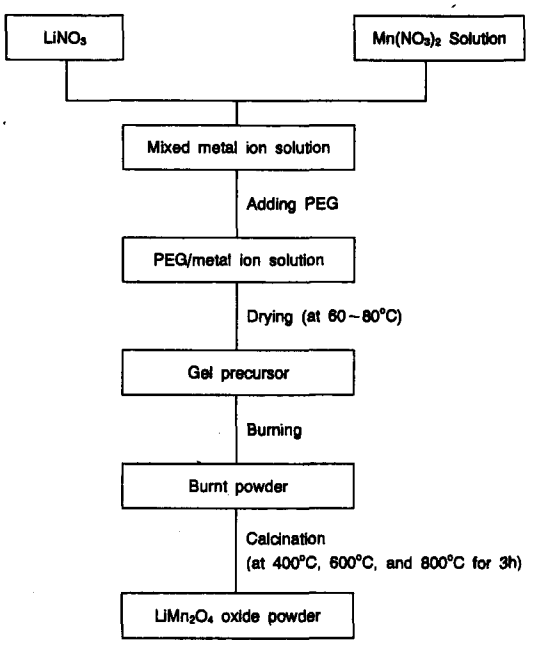

Figure 1. Flow chart for preparation of $LiMn_2O_4$ powder using PEG.

$Mn(NO_3)_2$ solution (0.06 mol) were dissolved in water, and then PEG (0.15 mol of repeating unit, -(-CH_2CH_2O-)-) was added to the solution. The mixed solution was heated at 60-80 °C on a hot plate with stirring for one day in order to evaporate excess water. As water evaporated, the solution became viscous and finally was transformed into a very viscous gel precursor with pale brown color.

The resultant precursor was ignited by a small gas flame at room temperature in air. Once the ignition started at a part of the bulk precursor, a weak flame spontaneously propagated through the bulk of the precursor, like a burning fuse. This burnt powder was calcined at 400, 600, and 800 °C for 3 h, respectively, in air to improve the crystallinity of product and also to allow the investigation of the formation route of the spinel $LiMn_2O_4$ phase.

Thermogravimetric analysis (TGA) and differential scanning calorimetry (DSC) were performed at a heating rate of 10 °C/min under static air and flowing nitrogen atmospheres with TGA-1000 and DSC-1500 instruments from Stanton Redcroft Co. X-ray diffraction (XRD) patterns of powders were taken with a Rigaku D-Max III diffractometer using Cu K_α radiation to characterize crystalline phases of the obtained powders. FT-IR spectra of pressed pellets with KBr were measured by using a Bomem MB-102 spectrometer. Elemental analysis was carried out by Carlo-Erba EA1108 elemental analyser to determine the residual amounts of elemental C, H, and N in the obtained powders. To investigate the characteristics of powders, scanning electron micrographs (SEM) were taken with a Hitachi S-4100 microscope and particle size distribution was measured by Cilas-Alcatel HR850 granulometer in water.

Results and Discussion

PEG was used to enhance the homogeneous mixing of the metal ions and suppress the precipitation of metal ni-

trates. Since PEG has electronegative ether oxygens in its chain, it can interact with electropositive metal ions.[24] This interaction and the random arrangement of polymer chain possibly enhance the mixing of metal ions. Thus lithium and manganese metal ions can be trapped homogeneously on a molecular scale throughout a polymeric matrix by the ion-dipole interaction. Such a structure also eliminates the need for long-range diffusion during the formation of lithium manganese oxides. Therefore, at a relatively low temperature the precursor can form a homogeneous single phase of precise stoichiometry. In addition, PEG can serve as a fuel at burning stage, being oxidized by the nitrate ions, and thus cause auto-ignited combustion of the precursor.

Thermal Analysis of the Precursor. The thermal decomposition of the gel precursor was investigated by DSC and TGA. The DSC curve of the precursor in air shows two large exothermic peaks at 173 and 265 °C, and also a small endothermic peak at about 130 °C, as shown in Figure 2(a). The TG curve (Figure 2(b)) of the precursor in air shows that a drastic weight loss occurs at about 175 °C, and two small losses at 130 and 259 °C. The small weight loss at 130 °C accompanied by a small endotherm might be ascribed to the evaporation of residual water. The two strong exothems are closely associated with the two weight losses. The abnormal drastic weight loss at 175 °C, which was accompanied by a sharp and intense exothemic peak,

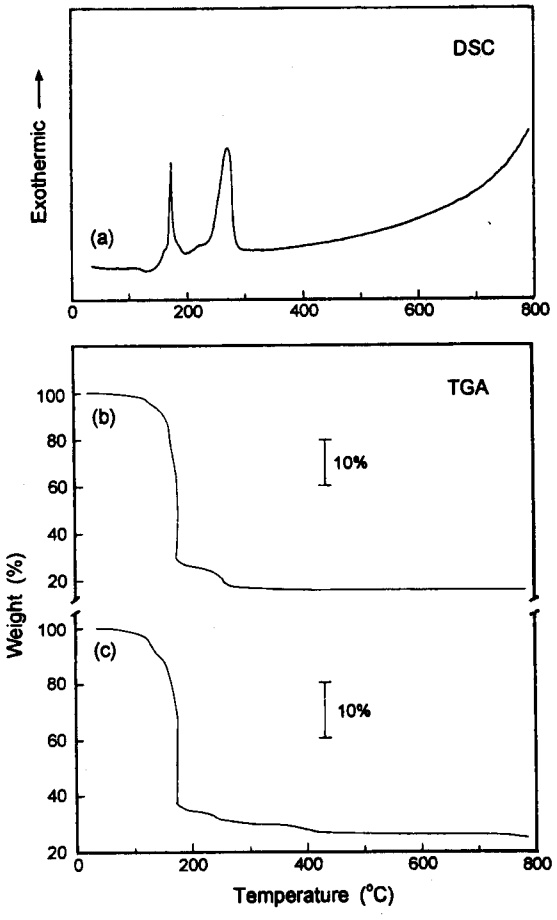

Figure 2. Thermal analysis of $LiMn_2O_4$ precursor. (a) DSC curve in static air, (b) TG curve in static air, and (c) TG curve in flowing nitrogen.

was not generally observed and only a few examples were reported in preparations of $La_{1-x}Sr_xMnO_3$[11,23] and $Bi_{1.75}Pb_{0.25}Sr_2Ca_2Cu_3O_{10+\delta}$ superconductor.[25] Furthermore, the TG curve (Figure 2(c)) under flowing nitrogen atmosphere shows that the weight loss occurs at about 175 °C irrespective of the oxygen partial pressure. Therefore, it supports that the thermal decomposition is an auto-ignited process and arises from a reaction between internal reactants coexisting in the precursor, without aid of oxygen gas. This thermal behavior of the precursor can be explained by recourse to the concepts of propellant chemistry used by Park *et al.*[11] and Patil *et al.*[18-21] They applied the valence concept for condensed fuel-oxidizer mixtures proposed by Jain *et al.*[22] to the preparations of various metal oxides through combustion process. According to the concepts, the elements, C, H, Li, and Mn are considered as reducing agents with corresponding valences, +4, +1, +1, and +2, respectively. On the other hand, the element oxygen is considered as the oxidizing element with valence of −2. The valence of nitrogen is considered to be zero. Among the reaction species, the nitrates, $LiNO_3$ and $Mn(NO_3)_2$, with oxidizing valence of −5 and −10 and the repeating unit of PEG, -(-CH_2CH_2O-)-, with reducing valence of +10 can act as an oxidizing agent (oxidizer) and a reducing agent (fuel), respectively. In the case of the gel precursor prepared in this study, the calculated ratio of reducing valence to oxidizing valence is 2.0, indicating that it is in fuel-rich condition. Since the oxidizer coexists closely with the fuel in a homogeneously mixed state, the nitrates can explosively react with the PEG with emitting large heat within a very short period when the precursor is heated to the temperature at which the reaction can occur. Therefore, the combustion reaction can cause the sharp exothemic peak and the drastic weight loss due to the rapid decomposition of PEG and nitrate ions. In addition, the resulting heat can be expected to raise the temperature of the reaction system and affect the formation route of $LiMn_2O_4$ phase. The other strong exothermic peak associated with the small weight loss observed at higher temperature may be due to the combustion of residual organic components derived from excess PEG.

Formation Route of $LiMn_2O_4$. XRD patterns (Figure 3) were taken to identify the formation of crystalline phases with increasing calcination temperature. In the burnt powder, the XRD pattern exhibits that some minor phases, such as MnO (JCPDS 7-230, manganosite), and Mn_3O_4 (JCPDS 24-734, hausmannite) [or γ-Mn_2O_3 (JCPDS 18-803)], coexists with the main phase of $LiMn_2O_4$ (JCPDS 35-782). It is difficult to discriminate between Mn_3O_4 and Mn_2O_3, since the two phases are known to have very similar XRD patterns and the obtained XRD pattern shows only very weak and broad peaks. A single phase of $LiMn_2O_4$ was obtained after calcination at 400 °C for 3 h and maintained up to 800 °C. The minor phases totally disappear after the calcination at 400 °C. Among these intermediate phases, MnO with a lower Mn valence, +2, has not been found in other reports on the preparation of $LiMn_2O_4$. The peaks of $LiMn_2O_4$ gradually sharpen with increasing calcination temperature, which indicates a growth of crystallite.

IR spectra of the precursor and the obtained powders are shown in Figure 4. The precursor shows many peaks, such

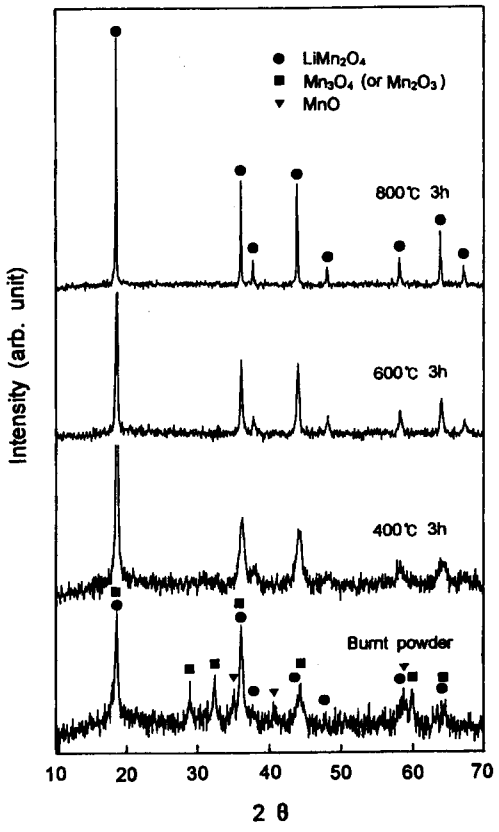

Figure 3. XRD patterns of burnt powder and calcined powders at 400 °C, 600 °C, and 800 °C for 3 h.

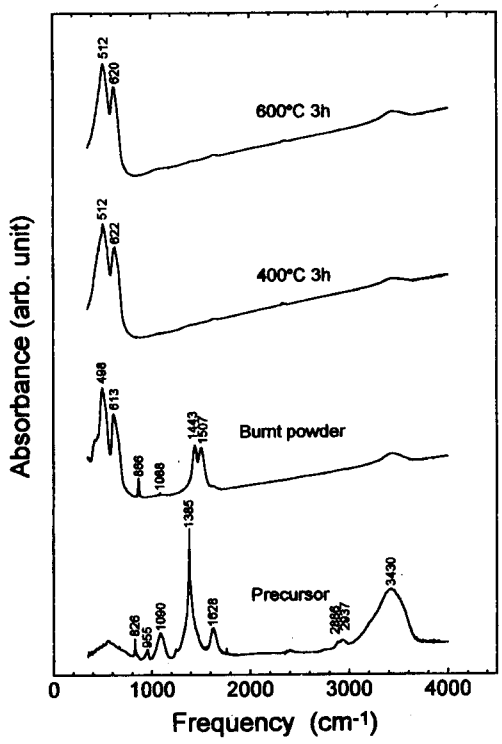

Figure 4. FT-IR spectra of precursor, burnt powder, and calcined powders at 400 °C and 600 °C for 3 h.

as stretching and bending band of residual water at 3430 and 1628 cm^{-1}, C-H stretching bands of PEG at about 2900 cm^{-1}, and a characteristic bands of NO_3^- at 1385 cm^{-1}. Besides these bands, many other complex bands corresponding to the stretching and the bending mode from PEG and NO_3^- ion are observed below 1500 cm^{-1}.[26-28] The burnt powder shows bands at 1507, 1443, 1088, and 866 cm^{-1}, believed to be due to carbonate ion CO_3^{2-}.[26,27] Considering the facts that any XRD peaks of crystalline metal carbonates were not detected and Li have much lower X-ray scattering power than Mn, the carbonate is probably expected to be amorphous type or Li_2CO_3. The bands below 700 cm^{-1} are presumably due to metal oxide and carbonate. However, the carbonate bands disappear by the subsequent calcination at 400 °C and only two bands at 512 and 622 cm^{-1} remained (the bands observed at 3430 and 1628 cm^{-1} are due to water absorbed in KBr). The IR spectrum of the calcined powders fully agrees with that of $LiMn_2O_4$ reported by Wen *et al.*[29]

The burnt powder contained some impurity oxide phases, such as MnO and Mn_3O_4 (or Mn_2O_3) with lower oxidation states of Mn than that of $LiMn_2O_4$. It has been well known that the oxidation state of Mn in oxide-type compounds is dependent on both temperature and partial pressure of oxygen; it decreases as the temperature increases and the partial pressure of oxygen decreases.[30,31] According to the phase diagram determined by using calorimetry,[31] MnO_2 is stable below about 410 °C, Mn_2O_3 between 410 and 710 °C, Mn_3O_4 beyond 710 °C, and MnO in much higher temperature region in air. In the burning process, the reaction of an oxidizer with a fuel emitted large heat leading to the increase of the temperature of the reaction system. Furthermore, the CO gas having reducing power can be produced by incomplete combustion of PEG. Consequently, the two factors can cooperatively suppress the oxidation of Mn^{2+} to Mn^{3+} (or Mn^{4+}) and manganese oxides with lower Mn oxidation states were formed during the burning process. If oxygen is supplied from air in sufficient quantity during the subsequent calcination at 400 °C, the impurity oxides with lower Mn oxidation states were then converted into the more stable $LiMn_2O_4$ with higher Mn oxidation states. The burnt powder also included a carbonate-type compound as another impurity phase. The metal carbonate can be formed by the reaction of Li or Mn ion with CO_2 gas evolved from the combustion of PEG. Since the IR spectrum of the burnt powder is similar to that of Li_2CO_3, it can be presumably expected that Li_2CO_3 is mainly produced.[27]

Based on the observed experimental results, a tentative reaction path for the formation of the $LiMn_2O_4$ phase including the possible intermediate phase formations may be proposed as follows:

PEG-Metal nitrate precursor
↓ Burning
$LiMn_2O_4$+minor phases (MnO, Mn_3O_4 (or Mn_2O_3), and carbonate)
↓ Calcination at 400 °C
$LiMn_2O_4$ with low crystallinity
↓ Further calcinations at 600 and 800 °C
$LiMn_2O_4$ with high crystallinity

Table 1. Results of Elemental Analysis for Burnt and Calcined Powders

Element	Burnt powder	Calcination temperature (°C)		
		400	600	800
Carbon	2.37	0.19	0.18	–
Nitrogen	–	–	–	–
Hydrogen	–	–	–	–

– : below detection limit.

Characterization of $LiMn_2O_4$ Powder. Unlike in the solid state reaction, it was anticipated that some carbon residue could remain in $LiMn_2O_4$ prepared at low temperatures, especially when an organic polymer was used as the gelling agent. In order to know how much carbon exists in the obtained powders, elemental analysis was carried out. Results are illustrated in Table 1. After burning the precursor, elemental carbon of 2.37% was present. By subsequent calcinations the carbon residue was almost removed from the powders. For all the samples, the contents of nitrogen and hydrogen was below the detection limit. It is suggested that the NO_3^- ions and the organic component from PEG totally decomposed at the burning stage. Therefore, the carbon detected by the elemental analysis can exist mainly as a form of carbonate, as supported by the IR spectrum of the burnt powder.

The DSC and TG analysis of the burnt powder were also performed and are shown in Figure 5. In the DSC curve no significant peak was observed, whereas the TG curves show weight losses of about 9.4% in nitrogen atmosphere and about 2.8% in air between 25 and 425 °C. Since any organic component is not present in the burnt powder as described above, it can be suggested that the weight losses in TG curves are probably caused by decompositions of the carbonate-type compound. Therefore, it can be calculated that the carbon content of 2.37% observed from the elemental analysis corresponds to weight loss of 11.8% in TG curve. The obtained values of weight losses of 9.4% in nitrogen and 2.8% in air, are lower than the calculated value of 11.8%. In the subsequent calcination process, the lacking amount of oxygen, which is required for the oxidation of Mn, should be supplied from oxygen sources such as carbonate anion or air. During this process, the carbonate present in the burnt powder is able to react with manganese oxides having lower Mn oxidation state to form $LiMn_2O_4$ having higher Mn oxidation state. The weight loss in nitrogen is larger than that in air because oxygen cannot be supplied from atmosphere. Therefore, it is clear that the carbon present in the burnt powder is mainly carbonate type and also the weight losses in TG curves mainly result from the decomposition of the carbonate.

SEM photographs of the powders obtained by calcinations at 400 and 800 °C for 3 h are shown in Figure 6. The product consists of very fine particles and the particle sizes are ~100 and ~500 nm for the samples calcined at 400 and 800 °C, respectively. However, the powders are shown to be highly agglomerated. In order to check the degree of agglomerization, particle size analysis was performed and the results are illustrated in Figure 7. It appears from the dis-

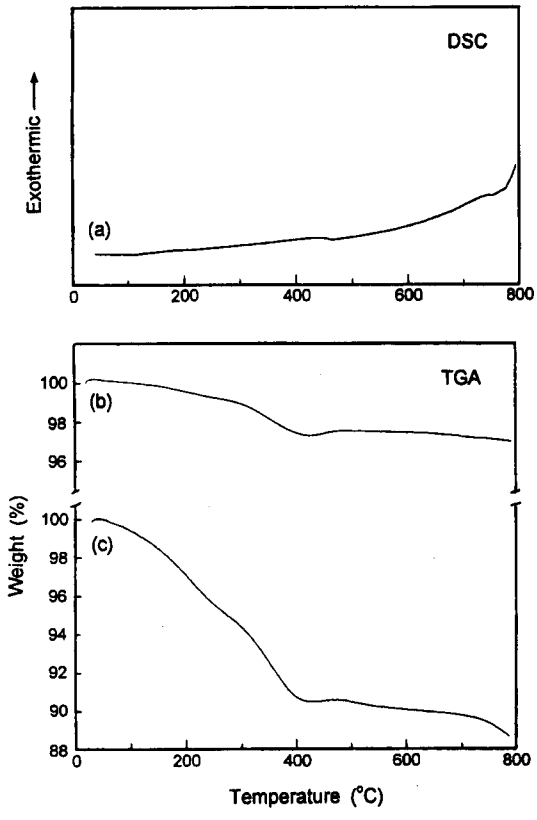

Figure 5. Thermal analysis of burnt powder. (a) DSC curve in static air, (b) TG curve in static air, and (c) TG curve in flowing nitrogen.

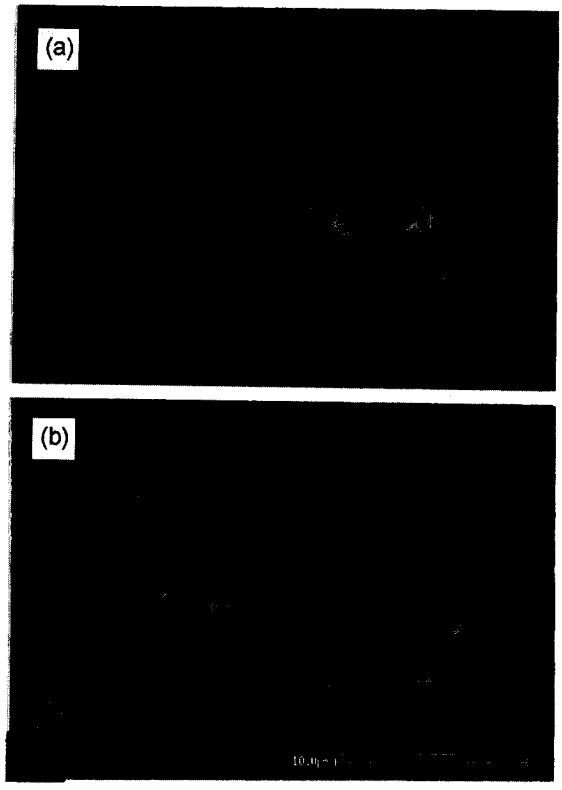

Figure 6. SEM photographs of $LiMn_2O_4$ powders calcined at (a) 400 °C and (b) 800 °C for 3 h.

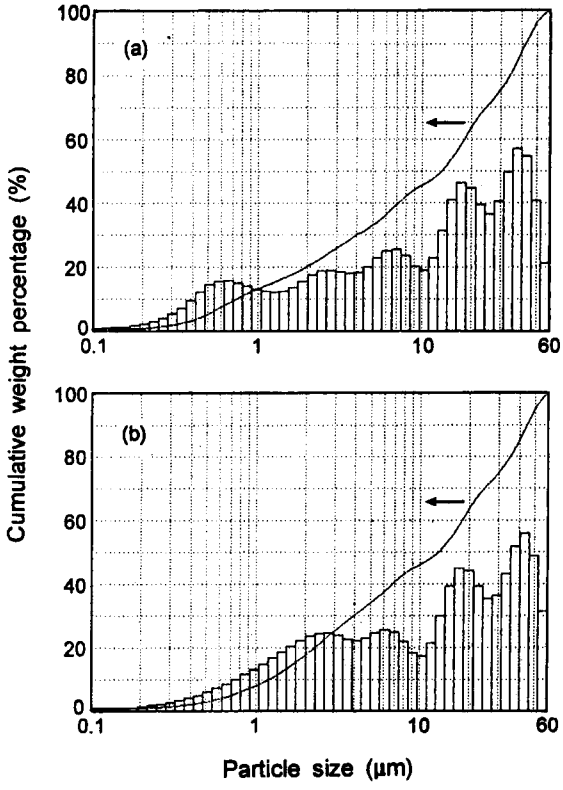

Figure 7. Particle size distributions and cumulative weight percentage c urves of $LiMn_2O_4$ powders calcined at (a) 400 °C and (b) 800 °C for 3 h.

tribution of particle size that both powders calcined at 400 °C and 800 °C show very broad particle size distributions and the contents of particles larger than 10 μm in diameter are more than 50%. These results are in agreement with the fact that the particles are highly agglomerated as observed in SEM micrographs. By comparing the parts below 4 μm, a difference in particle size distribution can be seen. With the increase of calcination temperature from 400 to 800 °C, the content of particles smaller than 1 μm reduced probably because of sintering between the individual particles. This phenomenon is consistent with the decrease in peak-width observed in XRD patterns with increasing calcination temperature.

Summary

$LiMn_2O_4$ powder was successfully prepared from the decomposition of PEG-metal nitrate gel precursor at low temperature of 400 °C. In thermal analysis of the precursor, a drastic weight loss, which was accompanied by a sharp and large exothemic peak, was observed at 175 °C. This abnormal thermal behavior could be explained in terms of the violent reaction between an oxidizer (nitrates) and a fuel (PEG) by employing the valence concepts of propellant chemistry. It was found that a single phase of $LiMn_2O_4$ was produced by calcinations above 400 °C, *via* an intermediate state containing minor phases such as manganese oxides with lower valent Mn ions and carbonate. The formation of minor phases at burning stage could be explained in terms of the heat and reducing atmosphere produced by the violent reaction between oxidizer and fuel coexisting in the precursor. The obtained powders were composed of submicron-sized particles, but highly agglomerated and thus showed broad particle size distributions.

Acknowledgment. This work was supported by the Post-Doc. Program of The Institute of Basic Science of Korea University.

References

1. Koksbang, R.; Barker, J.; Shi, H.; Saïdi, M. Y. *Solid State Ionics* **1996**, *84*, 1.
2. Tarascon, J. M.; Guyomard, D. *Electrochimica Acta* **1993**, *38*, 1221.
3. Ohzuku, T.; Kitagawa, M.; Hirai, T. *J. Electrochem. Soc.* **1990**, *137*, 769.
4. Masquelier, C.; Tabuchi, M.; Ado, K.; Kanno, R.; Kobayashi, Y.; Maki, Y.; Nakamura, O.; Goodenough, J. B. *J. Solid State Chem.* **1996**, *123*, 255.
5. Momchilov, A.; Manev, V.; Nassalevska, A. *J. Power Sources* **1993**, *41*, 305.
6. Barboux, P.; Tarascon, J. M.; Shokoohi, F. K. *J. Solid State Chem.* **1991**, *94*, 185.
7. Huang, H.; Bruce, P. G. *J. Electrochem. Soc.* **1994**, *141*, L106.
8. Liu, W.; Farrington, G. C.; Chaput, F.; Dunn, B. *J. Electrochem. Soc.* **1996**, *879*, 1591.
9. Pechini, M. P. *U. S. Patent* No. 3330697, July 11, 1967.
10. Li, X.; Zhang, H.; Chi, F.; Li, S.; Xu, B.; Zhao, M. *Mater. Sci. Eng. B* **1993**, *18*, 209.
11. Park, H.-B.; Kweon, H.-J.; Hong, Y.-S.; Kim, S.-J.; Kim, K. *J. Mater. Sci.* **1997**, *32*, 57.
12. Kweon, H.-J.; Kuk, S.-T.; Park, H.-B.; Park, D. G.; Kim, K. *J. Mater. Sci. Lett.* **1996**, *15*, 428.
13. Saha, S. K.; Pathak, A.; Pramanik, P. *J. Mater. Sci. Lett.* **1995**, *14*, 35.
14. Lessing, P. A. *Am. Ceram. Soc. Bull.* **1989**, *68*, 1002.
15. Taguchi, H.; Matsuda, D.; Nagao M. *J. Am. Ceram. Soc.* **1992**, *75*, 201.
16. Taguchi, H.; Yoshioka, H.; Matsuda, D.; Nagao, M. *J. Solid State Chem.* **1993**, *104*, 460.
17. Sun, Y.-K.; Oh, I.-H.; Hong, S.-A. *J. Mater. Sci.* **1996**, *31*, 3617.
18. Manoharan, S. S.; Patil, K. C. *J. Am. Ceram. Soc.* **1992**, *75*, 1012.
19. Suresh, K.; Patil, K. C. *J. Solid State Chem.* **1992**, *99*, 12.
20. Manoharan, S. S.; Patil, K. C. *J. Solid State Chem.* **1993**, *102*, 267.
21. Chandran, R. G.; Patil, K. C.; Chandrappa, G. T. *J. Mater. Sci.* **1996**, *31*, 5773.
22. Jain, S. R.; Adiga K. C.; Verneker, V. R. P. *Combustion and Flame* **1981**, *40*, 71.
23. Chakraborty, A.; Devi, P. S.; Maiti, H. S. *Mater. Lett.* **1994**, *20*, 63.
24. Okada, T. *Analyst* **1993**, *118*, 959.
25. Devi, P. S.; Maiti, M. S. *J. Solid State Chem.* **1994**, *109*, 35.
26. Ross, S. D. *Inorganic Infrared and Raman Spectra*; McGraw-Hill Book Company: London, U.K., 1972.
27. Nyquist, R. A.; Kagel, R. O. *Infrared Spectra of Inor-*

ganic Compounds; Academic press: New York, U.S.A., 1994.
28. Pavia, D. L.; Lampman, G. M.; Kriz Jr., G. S. *Introduction to Spectroscopy*; W. B. Saunders Company: Philadelphia, U.S.A., 1979.
29. Wen, S. J.; Richardson, T. J.; Ma, L.; Striebel, K. A.; Ross Jr, P. N.; Cairns, E. J. *J. Electrochem. Soc.* **1996**, *143*, L136.
30. Duval, C. *Inorganic Thermogravimetric Analysis*, 2nd ed; Elsevier Publishing Company: London, U.K., 1963.
31. Fritsch, S.; Navrotsky, A. *J. Am. Ceram. Soc.* **1996**, *79*, 1761.

Syntheses of Polysiloxane-Bridged Dinuclear Metallocenes and Their Catalytic Activities

Seok Kyun Noh*, Suchan Kim, Dong-ho Lee*†, Keun-byoung Yoon†, and Hun-bong Lee†

School of Chemical Engineering and Technology, Yeungnam University, 214-1 Tae-dong, Kyongsan 712-749, Korea
†Department of Polymer Science, Kyungpook National University, Taegu 702-701, Korea
Received March 11, 1997

The polysiloxane-bridged dinuclear metallocenes $[(SiMe_2O)_n\text{-}SiMe_2(C_5H_4)_2][(C_9H_7)ZrCl_2]_2$ (n=1 (**7**), 2 (**8**), 3 (**9**)) have been generated as a model complex for the immobilized metallocene at silica surface by treating the respective disodium salts of the ligands with 2 equivalents of $(C_9H_7)ZrCl_3$ in THF. All three complexes are characterized by ^1H NMR and measurement of metal content through ICP-MS. It turned out that the values of $\Delta\delta=[\delta_d\text{-}\delta_p]$, the chemical shift difference between the distal (δ_d) and proximal (δ_p) protons, for the produced dinuclear compounds (0.47 for **7**, 0.49 for **8**, and 0.5 for **9**) were larger than the $\Delta\delta$ value of the known *ansa*-type complex holding the same ligand as a chelating one, that is just the opposite to the normal trend. In order to compare polymerization behavior of the dinuclear metallocene with the corresponding mononuclear metallocene, $(Cp)(C_9H_7)ZrCl_2$ was separately prepared. To investigate the catalytic properties of the dinuclear complexes and mononuclear metallocenes ethylene polymerization has been conducted in the presence of MMAO. The polymerization results display the typical activity dependence on polymerization temperature for all complexes. The most important feature is that the polymers from the dinuclear metallocenes represent enormously improved molecular weight compared with the polymer from the corresponding mononuclear metallocene. In addition, the influence of the nature of the bridging ligand upon the reactivities of the dinuclear metallocenes has also been observed.

Introduction

Since the discovery in 1980 that in the presence of MAO Cp_2ZrCl_2 acts as a homogeneous catalyst for ethylene polymerization, many efforts have been devoted to the development of various kinds of metallocenes that not only polymerize α-olefins but also polymerize polar monomers.[1] As a consequence there have been very valuable advances on both academic and industrial sides that allow a better understanding of the polymerizaton mechanism and of the correlation between metallocene structure and polymer properties.[2]

We have been interested in preparing metallocenes containing the polysiloxane moiety and probing their polymerization behaviors, since these compounds could be an adequate model to study the reactivities of an immobilized metallocene at the silica surface. Recently we reported the synthesis of polysiloxane-bridged *ansa*-metallocene[3] as well as dinuclear half-metallocenes[4] having two $[CpTiCl_3]$ fragments, and their polymerization results. In particular, dinuclear metallocenes have attracted attention because the two metal centers may show cooperative electronic and chemical effects which could be potentially useful for the development of new metallocene catalysts. Furthermore, it is plausible that the dinuclear metallocene complexes might be a better model to investigate characteristics of an immobilized metallocene than the corresponding mononuclear metallocene, because the immobilized metallocene could be regarded as a kind of multinuclear metallocene, as shown in Figure 1.

Recently, Patterson prepared a series of dinuclear zirconocene complexes $[X(C_5H_4)_2][(C_5R_5)ZrCl_2]_2$ (X=CH_2, $SiMe_2$; R=H, CH_3), which contain two mechanically linked zirconocene dichloride units and examined the structural response of the $[SiMe_2(C_5H_4)_2]^{2-}$ ligand to changes in the metal coordination environment.[5] More recently, Royo described the synthesis and characterization of dinuclear metallocene complexes of titanium with $[SiMe_2(C_5H_4)_2]^{2-}$ as a bridging ligand.[6] Although some interesting dinuclear metallocene complexes of titanium and zirconium are well represented, relatively few publications have demonstrated the utilization of dinuclear metallocene as an olefin polymerization catalyst.[7]

We are especially interested in reactivity studies aiming at how the mutual participation of two metal centers modifies the reactivity patterns normally shown by the corresponding mononuclear fragments according to the nature